Long-range three-dimensional magnetic structures of the spin $S=1$ hexamer cluster fedotovite-like $A_2Cu_3O(SO_4)_3$ ($A_2=K_2$, NaK, Na$_2$): A neutron diffraction study

V. Yu. Pomjakushin

Laboratory for Neutron Scattering and Imaging LNS, Paul Scherrer Institut, CH-5232 Villigen PSI, Switzerland

A. Podlesnyak

Neutron Scattering Division, Oak Ridge National Laboratory, Oak Ridge, Tennessee 37831, USA

A. Furrer

Laboratory for Neutron Scattering and Imaging LNS, Paul Scherrer Institut, CH-5232 Villigen PSI, Switzerland

E. V. Pomjakushina

Laboratory for Multiscale Materials Experiments LMX, Paul Scherrer Institut, CH-5232 Villigen PSI, Switzerland

The crystal and magnetic structures of the spin $S = 1$ hexamer cluster fedotovite-like $A_2Cu_3O(SO_4)_3$ ($A_2 = K_2$, NaK, Na$_2$) were studied by neutron powder diffraction at temperatures 1.6–290 K. The crystal structures in all compounds are well refined in the monoclinic space group C2/c. The basic magnetic units of the compounds are copper hexamers, which are coupled by weak superexchange interactions giving rise to three-dimensional long-range magnetic order below $3.0 < T_N < 4.7$ K. We have found that for $A_2 = K_2$ and NaK the propagation vector of the magnetic structure is $\bm{k} = [0, 0, 0]$, and the coupling of the Cu hexamers is ferromagnetic (FM) along the *ab* diagonal and antiferromagnetic along the *bc* diagonal. In contrast, for $A = $ Na the propagation vector is $\bm{k} = [0, 1, 0]$, and the Cu hexamers are coupled antiferromagnetically (AFM) along the *ab* diagonal. The hexamers are formed by three Cu pairs arranged along the *b* axis. The calculated spin expectation values $\langle s \rangle$ for the simplest symmetric spin Hamiltonian (obtained from inelastic neutron spectroscopy) of the isolated hexamers in the mean field amounted to $\langle s \rangle = 3/8$ for the side spins Cu1 and Cu2 and $\langle s \rangle = 1/4$ for Cu3 in the middle. The Cu spins are FM coupled in pairs and AFM between neighboring pairs. The experimental magnetic moments of the Cu^{2+} ions turn out to be not completely collinear due to spin frustrations within the weak interhexamer interactions. The sizes of magnetic moments of Cu in the hexamers determined from the diffraction data are in fair agreement with the calculated values.

DOI: 10.1103/PhysRevB.109.144409

I. INTRODUCTION

Quantum magnetism and related spin frustration phenomena are relevant topics in the present surge of interest in condensed-matter physics. Of particular importance are studies of spin $S = 1/2$ systems, in which spin frustration is often present due to both quantum spin fluctuations and the lack of anisotropy. Such phenomena have been observed in many compounds and particularly in compounds built up of magnetic clusters that interact as single magnetic units in the three-dimensional lattice [1,2]. Their magnetic properties are governed by strong intracluster and weak intercluster interactions, so that the interplay of different energy scales and dimensionalities can lead to unusual phenomena. More recently, an increasing number of investigated compounds benefited from observations on naturally occurring minerals [2,3], thereby bridging mineralogy with condensed-matter physics. Here we focus on the minerals $A_2Cu_3O(SO_4)_3$ (punite $A = $ Na, euchlorine $A_2 = $ NaK, fedotovite $A_2 = $ K$_2$), which have been studied in the past few years by a variety of both experimental and theoretical methods [4–10]. The compounds are built up of edge-shared tetrahedral spin clusters consisting of three pairs of Cu^{2+} ions with spin $S = 1/2$ forming quasi-isolated hexamers as shown in Fig. 1. The intracluster interactions result in a triplet ground state $S = 1$ for the copper hexamers [4,6,8], which are weakly coupled giving rise to long-range magnetic order below $T_N = 3.4$ K ($A = $ Na), 4.7 K ($A_2 = $ NaK), and 3.0 K ($A = $ K) [9], thereby challenging the earlier description of the title compounds in terms of Haldane spin chains [3]. Later studies gave evidence for two-dimensional superexchange interactions within the *bc* plane [9,10]. So far detailed information on the magnetic structures is missing, except from a neutron diffraction study performed for $A = $ K, where the solution was found in Shubnikov group C2'/c with the moments aligned in the *ac* plane [7]. We would like to emphasize that the magnetic neutron diffraction experiments in this system are very difficult because of the small magnetic moments of the Cu^{2+} spin $S = 1/2$ and very large natural background due to the fact that the magnetic intensities are positioned on top of huge nuclear Bragg peaks. The nuclear peaks are contributed by 168 atoms, whereas the magnetic peaks are formed only by 24
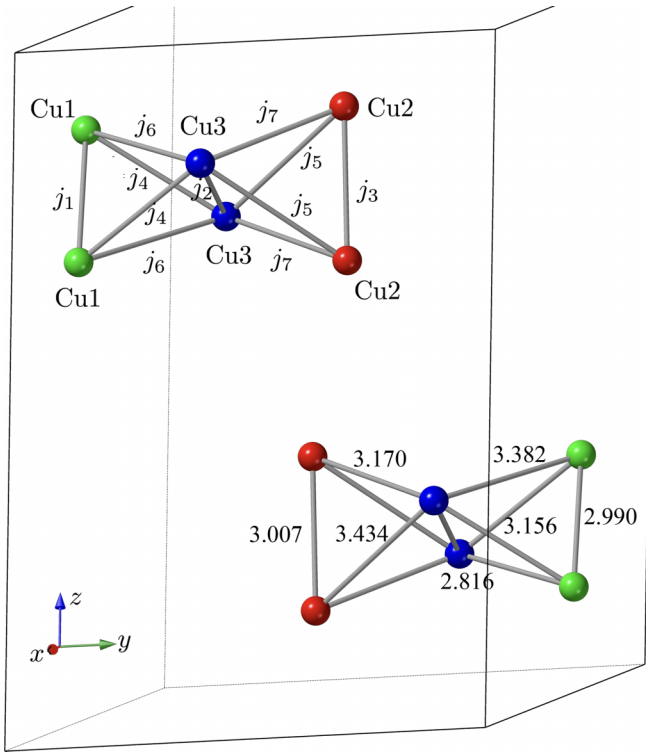
FIG. 1. Two Cu hexamers out of four in the unit cell are shown for the $A_2 = $ NaK sample. For better visibility, some atoms in hexamers are extended to neighboring cells. The hexamers are related by inversion. Two other hexamers, which are not shown, are related by C-centering translation (1/2, 1/2, 0). The bond lengths in Å are indicated for the bottom hexamer. J_i ($i = $ 1–7) show the exchange coupling constants used in Sec. IV and in Eq. (1).

Cu spins per unit cell. In Ref. [4], no magnetic Bragg peaks were detected in the neutron powder diffraction experiment down to 1.6 K in the sample with $A = $ K. Hase *et al.* [7] have successfully found the solution for the magnetic structure for $A = $ K from a relatively low number of diffraction peaks with only one statistically relevant magnetic reflection. The nonzero magnetic moments were found only at the side Cu pairs Cu1 and Cu2 in the hexamer.

The present work reports on the magnetic structures determined from neutron diffraction experiments carried out below and above T_N. We find that the compounds with $A_2 = $ K$_2$ and NaK are defined by the magnetic Shubnikov group C2'/c (No. 15.87, BNS). The propagation vector is $\boldsymbol{k} = [0, 0, 0]$, and the coupling of the Cu hexamers is ferromagnetic along the *ab* diagonal. In contrast, for $A = $ Na the magnetic Shubnikov group is C_P2'/c (OG symbol [11]) or P_C2_1/c (No. 14.84, BNS) with propagation vector $\boldsymbol{k} = [0, 1, 0]$, and the Cu hexamers are coupled antiferromagnetically along the *ab* diagonal. All Cu atoms in hexamers have nonzero magnetic moment values. Our results are discussed in terms of the intrahexamer and interhexamer exchange parameters available for the title compounds [9,10]. Spin frustration turns out to be evident, which is actually expected from the empirical quantity $|T_{cw}/T_N| \gg 1$ [12], where T_{cw} is the Curie-Weiss temperature derived from magnetic susceptibility measurements [9]. The experimental observation of the 3D long-range magnetic order seems to

forbid the emergence of the cluster-based Haldane state in this system.

II. SAMPLES SYNTHESIS AND EXPERIMENTAL DETAILS

Polycrystalline samples of $A_2Cu_3O(SO_4)_3$ ($A_2 = $ Na, K$_2$, and NaK) were synthesized by a solid-state reaction process. High-purity CuO, CuSO$_4$, and A_2SO$_4$ ($A = $ Na, K) were mixed in a molar ratio 1:2:1, followed by annealing at 500 °C, 580 °C, and 480 °C in air (for Na, K, and NaK, respectively) for at least 100 h with intermediate grindings. The samples were characterized by x-ray and neutron diffraction confirming their single-phase character.

Neutron scattering measurements for the magnetic structure determination were performed at the time-of-flight Cold Neutron Chopper Spectrometer (CNCS) [13] at the Spallation Neutron Source (SNS) at Oak Ridge National Laboratory (USA). The samples were enclosed in aluminum cylinders (8-mm diameter, 45-mm height) and placed into an orange cryostat. The data were collected using fixed incident neutron wavelength $\lambda = 4.96$ Å. For the crystal structure studies, we used the high-resolution diffractometer for thermal neutrons HRPT [14] with a wavelength 2.45 Å at the SINQ spallation source at the Paul Scherrer Institute (Switzerland). The determination of the crystal and magnetic structure parameters was done using the FULLPROF [15] program, with the use of its internal tables for the neutron scattering lengths. The symmetry analysis was performed using ISODISTORT from the ISOTROPY software [16,17] and some software tools of the Bilbao crystallographic server such as MVISUALIZE [18,19].

III. CRYSTAL STRUCTURE

The crystal structures in all samples $A_2Cu_3O(SO_4)_3$ ($A_2 = $ NaK, K$_2$, Na$_2$) are well refined in the monoclinic space group C2/c (No. 15) from the HRPT data with the example of the diffraction pattern and its Rietveld refinement shown in Fig. 2. The structure parameters are listed in the supplementary materials in Tables S1 and S2 in Refs. [6] and [10], respectively. Here we present in Table I only the crystal metrics and the Cu positions relevant for the present paper. The full structure information can be found in magnetic crystallographic information files (mcif) in the Supplemental Material [20]. The initial values of the structure parameters were taken from the x-ray diffraction results [21,22]. The structure parameters refined from our neutron powder diffraction data are in good agreement with those obtained from x-ray data. The crystal structure is illustrated in Fig. 3. It is quite complex and contains 168 atoms in a unit cell, making it not so easy to visualize. The structure contains 20 atoms in the general 8f position and two oxygen atoms in the special 4e position with 62 positional parameters to refine.

One unit cell contains 24 Cu atoms forming four Cu hexamers, two of which are shown in Fig. 1. Each hexamer has 2-fold axis symmetry and formed by Cu1, Cu2, and Cu3 pairs. The atoms in the pairs are related by a 180-degree rotation around the y axis ($\{2_y|00\frac{1}{2}\}$ operator in C2/c). The second hexamer is related to the first one by two other symmetry operators -1 and $\{m_y|00\frac{1}{2}\}$.

The diffraction patterns measured at CNCS with large neutron wavelength are limited by the Q range ($Q_{max} = 2.3$ Å^{-1})

TABLE I. The structure parameters in $A_2Cu_3O(SO_4)_3$ (A_2 = K_2, NaK, Na_2) at $T = 2$ K in the parent space group C2/c: lattice parameters a, b, c, β, and fractional atomic coordinates x, y, z. The positions of Cu are the same in the magnetic space group (MSG) 15.87 C2'/c for A_2 = K_2, NaK. For A = Na the MSG is 14.84 P2_1/c.1'_C[C2/c] (UNI symbol); the Cu positions are different due to origin shift and given on a separate line. All atoms are in the Wyckoff positions (8f). Only the Cu atom coordinates are presented that are relevant for the analysis of the magnetic diffraction patterns. The conventional reliability factors [15] R_p, R_{wp}, R_{exp}, χ^2 are also given. The parameters were refined from the powder neutron diffraction patterns measured at HRPT/SINQ with wavelength $\lambda = 2.45$ Å.

	$A_2 = K_2$	A_2 = NaK	$A_2 = Na_2$
a (Å)	18.9755(7)	18.4730(8)	17.2141(7)
b (Å)	9.5004(4)	9.3644(4)	9.3729(4)
c (Å)	14.1972(5)	14.3146(6)	14.3701(5)
β (deg)	110.4915(9)	113.9642(10)	111.8436(8)
V (Å^3)	2397.5(2)	2262.8(2)	2152.1(1)
Cu1 $x\,y\,z$	0.4813(3) 0.0227(5) 0.3403(3)	0.4827(3) 0.0205(6) 0.3430(4)	0.4774(2) 0.0202(5) 0.3406(3)
Cu2 $x\,y\,z$	0.4858(2) 0.4778(5) 0.1392(3)	0.4834(3) 0.4724(5) 0.1381(4)	0.4856(2) 0.4789(4) 0.1410(3)
Cu3 $x\,y\,z$	0.4199(3) 0.7451(7) 0.2055(4)	0.4166(3) 0.7483(7) 0.2043(3)	0.4123(3) 0.7475(5) 0.2017(3)
R factors	3.58 4.65 3.00 2.41	3.42 4.39 3.16 1.93	3.39 4.45 2.99 2.20
		A = Na, Cu positions in MSG P2_1/c.1'_C[C2/c]	
	Cu1 $x\,y\,z$	Cu2 $x\,y\,z$	Cu3 $x\,y\,z$
	0.2274 0.7702 0.3406	0.2356 0.2289 0.1410	0.6623 -0.0025 0.2017

so that, in the crystal structure fits, only the profile parameters and overall scale factor were refined to be used later for the magnetic structure fits. The fit quality is good for all three samples as illustrated for A_2 = NaK in Fig. 4.

IV. EXPECTATION VALUES OF $\frac{1}{2}$-SPINS IN AN ISOLATED HEXAMER

The Hamiltonian of the isolated hexamer reads

$$H = -2\sum_{i=1}^{7} J_i \mathbf{s} \cdot \mathbf{s}' - h_{mf}S_z, \qquad (1)$$
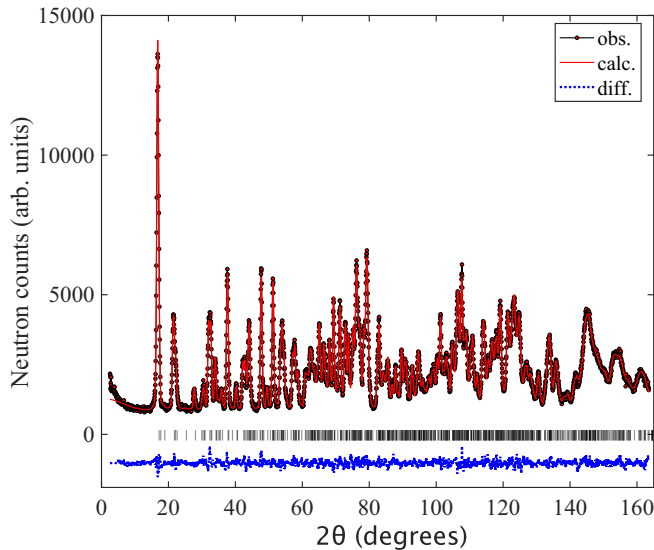

FIG. 2. The Rietveld refinement pattern and the difference plot between observed and calculated intensities of the neutron diffraction data for the sample $A_2Cu_3O(SO_4)_3$ (A_2 = NaK) at $T = 1.6$ K measured at HRPT with the wavelength $\lambda = 2.45$ Å. The row of tick marks shows the Bragg peak positions. The difference between observed and calculated intensities is shown by the dotted blue line.

where the sum runs over the exchange couplings J_i along the bonds in the hexamer as shown in Fig. 1, h_{mf} is the mean field, and S_z is the total spin projection of the hexamer molecule. Based on the results of inelastic neutron scattering (INS) studies [6,8,10], we have two models. The symmetric model with 4 parameters is solved exactly. In this case, the Hamiltonian has different J_1, J_3, J_2 between Cu1, Cu2, and Cu3 spin pairs and the same cross-exchange couplings J_5, J_6, J_7 equal to J_4. The four-parameter symmetric Hamiltonian is diagonalized algebraically with the explicit formula for the energy given by Formula (2) in Ref. [8] in the coupled basis with 5 quantum numbers, being the sums of spins in pairs Cu1, Cu2, Cu3, the sum of the pairs Cu1 and Cu2, and the total spin S.

The individual spins do not commute with the Hamiltonian, but the spin expectation values $\langle s \rangle$ are derived straightforwardly for the above pure quantum states through the Clebsh-Gordon coefficients and do not depend on the
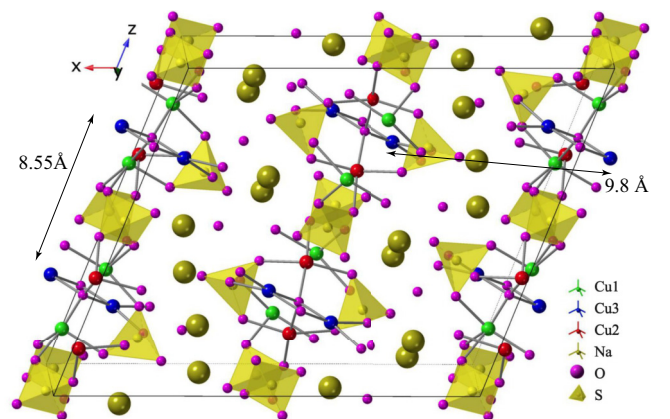

FIG. 3. The crystal structure in approximately one unit cell in the sample with A = Na. Six hexamers can be seen; polyatomic anions $(SO_4)^{2-}$ are shown as tetrahedra. The distances between tetramers are indicated. The connectivity between the hexamers is shown in more detail in Fig. 12.
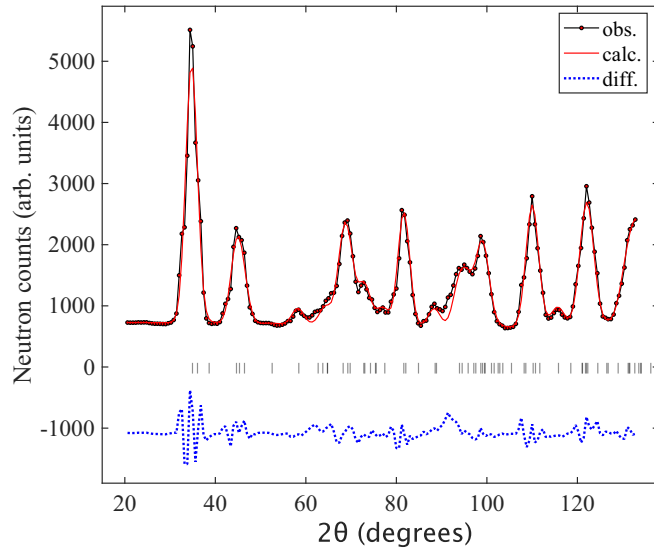
FIG. 4. The Rietveld refinement pattern and the difference plot between observed and calculated intensities of the neutron diffraction data for the sample $A_2Cu_3O(SO_4)_3$ $(A_2 = NaK)$ at $T = 6$ K at CNCS/SNS with the wavelength $\lambda = 4.96$ Å. All structure parameters were fixed by the values obtained from HRPT data (Fig. 2). The row of tick marks shows the Bragg peak positions. The difference between observed and calculated intensities is shown by the dotted blue line.

FIG. 5. The raw neutron diffraction patterns for the sample $A_2Cu_3O(SO_4)_3$ $(A = K)$ at $T = 1.6$ K (blue dotted line and open symbols), 6 K (red dashed line and closed symbols), and difference pattern containing purely magnetic contribution (black line and closed symbols), measured at CNCS/SNS with the wavelength $\lambda = 4.96$ Å. A constant 50 has been added to the difference pattern. Note, the *y* axis has logarithmic scale.

exchange constants J_i. Only the energy spectrum depends on the exchange parameters J_i. Here we use the basis of individual spins in the hexamer to calculate the expectation values of the spins to be later compared with the experiment for the general model of the Hamiltonian from INS experiments. In the spectrum, we have five singlets, nine triplets, five quintets, and one septet with the rational spin expectation values $\langle s \rangle$ of the Cu spins.

For the experimentally determined exchange parameters J_i $(i = 1$–$4)$ 1.2, 12.5, 2.3, and -6.7 meV for the sample with $A = $ Na [8], the ground state is a triplet and the next excited state is a singlet separated by the energy gap $2J_4 = 13.4$ meV. The mean field on the hexamer lifting up the degeneracy is less than $h_{mf} < 1.5$ meV [10] and does not mix the triplet wave function with the next singlet state one. The exchange parameters are slightly different for the samples with $A_2 = K_2$ and NaK, but the ground state is the same triplet with the spin expectation values $\langle s \rangle = \frac{3}{8}$ for the side Cu1 and Cu2, and $\langle s \rangle = -\frac{1}{4}$ for Cu3 in the middle for all three compositions. The spins in the Cu1, Cu2, and Cu3 pairs are coupled ferromagnetically (FM), and antiferromagnetically (AFM) between the middle Cu3 pair and the side Cu1 and Cu2 pairs with total hexamer spin $S_z = 1$. As we will show further in Sec. V B, this configuration is indeed observed experimentally with magnetic moment values in reasonable agreement with the above theoretical values. In the model with seven independent exchange parameters J_i $(i = 1$–$7)$: 1.3, 11.5, 2.2, $-8.3, -8.3, -4.7, -5.3$, refined from INS experiment [10], the Cu spins are coupled the same way. The Cu1, Cu3, and Cu2 spin expectation values $\langle s \rangle$ amounted to 0.395, -0.246, 0.351 similar to the symmetric model. The total hexamer spin
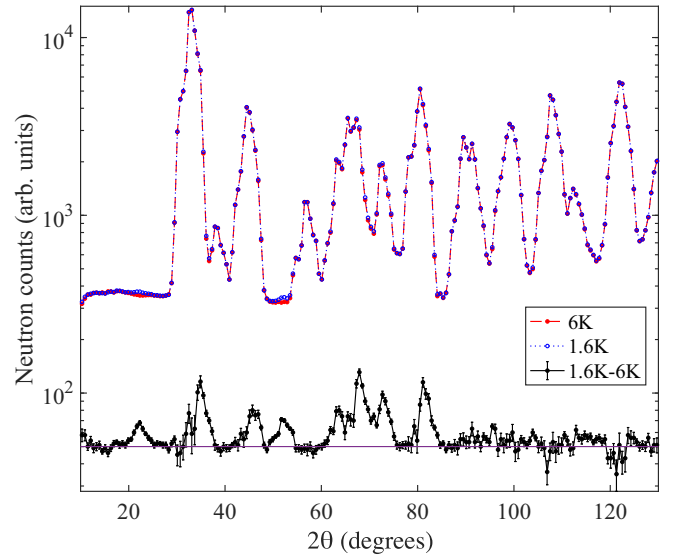
projection remains a good quantum number $S_z = 1$. The magnetic moment expectation values with the seven parameters from Ref. [10] are the same within the accuracy 0.005 μ_B for all three samples, being $2\langle s \rangle = 0.79, 0.49,$ and 0.70 μ_B for the Cu1, Cu3, and Cu2 magnetic moments. The FM coupling in the side pairs is actually not very sensitive to the small exchange parameters J_1 and J_3 in comparison with the large FM exchange J_2 in the middle Cu3-pair and interpair AFM exchanges J_i $(i = 4$–$7)$. The ground state will be the same triplet with FM pairs even if one flips the sign of the J_1 and J_3.

V. MAGNETIC STRUCTURES

The neutron diffraction intensities are dominated by very large nuclear peaks. One can see only subtle differences between base and paramagnetic temperatures in the raw neutron diffraction patterns shown in Fig. 5. The magnetic scattering is small and amounts to only less than about 0.5% in intensity as one can see from the figure. For this reason, the difference patterns, i.e., the difference between patterns taken at base $(\simeq 1.6$ K) and paramagnetic (6 K) temperatures, were used to solve and refine the magnetic structures. Such difference patterns contain purely magnetic scattering and are free of possible systematic uncertainties due to the fitting of large crystal structure Bragg peaks, background, impurities, etc.

The identification of the magnetic propagation vector was done using the so called Le Bail fitting, where all peak intensities are refined separately without any structure model, thus allowing a straightforward determination of the propagation vector **k**. In addition, this model-free fit defines the best possible goodness of fit. We have found that for the samples with $A_2 = K_2$ and NaK the propagation vector is **k** = 0 or the gamma point (GM) of the Brillouin zone (BZ)
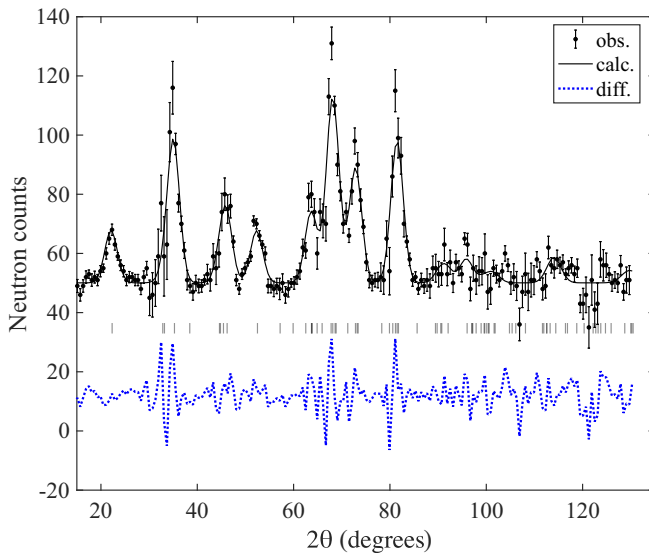
FIG. 6. The model-free Le Bail fit of the difference pattern for the sample $A_2Cu_3O(SO_4)_3$ (A = K) containing purely magnetic contribution, measured at CNCS/SNS with the wavelength $\lambda = 4.96$ Å. The row of tick marks shows the Bragg peak positions. The difference between the observed and calculated intensities is shown by the dotted blue line. The reliability factors [15] R_p, R_{wp}, R_{exp}, χ^2 are 6.15, 5.88, 4.65, 1.60.

(here we use internationally established nomenclature for the irreducible representations (irreps) labels and magnetic superspace groups MSSGs [16,18]). The fit quality for the sample with A = K is illustrated in Fig. 6. The total number of magnetic Bragg peaks is about 120. For the sample with A = Na, the propagation vector is $\boldsymbol{k} = [0, 1, 0]$ (Y point of BZ). The goodness of Le Bail fits is shown in Table II.

A. Symmetry analysis

The parent space group C2/c (No. 15) has four irreps for the gamma point GM [0,0,0] of the BZ. Since they are all one-dimensional real irreps, there are only four Shubnikov magnetic space subgroups (MSGs): mGM1+ 15.85 C2/c, mGM2+ 15.89 C2'/c', mGM1− 15.88 C2/c', mGM2− 15.87 C2'/c (we use the unified (UNI) MSG symbol [16,23]). The first two, which are inversion even (i.e., −1 is not primed), allow ferromagnetic (FM) ordering. For each MSG there are nine independent parameters to be determined experimentally. For the Y point [0,1,0] there are four irreps as well that generate four magnetic models in the MSGs 14.84 P2_1/c.1'_C[C2/c] and 13.74 P2/c.1'_C[C2/c] with two different basis transformations from the parent space group.

We present some more details for the MSG C2'/c (mGM2−), which is the solution that fits the neutron diffraction data very well for the samples with A_2 = K$_2$, NaK, and MSG P2_1/c.1'_C[C2/c] (mY2−) for the sample with A = Na, as shown in the next section, Sec. V B. In both cases there are 4 hexamers per unit cell (Figs. 1, 7), but the magnetic structure is defined by the magnetic configuration in a single hexamer.

The basis transformation to the C2'/c MSG structure is the identity matrix with the zero origin shift. The hexamers

are FM coupled in the *ab* plane because they are related by C-centering, which does not change the spin for the GM point. The coupling between the closest hexamers along the *bc* diagonal related by primed inversion −1' is AFM. The above interhexamer couplings are fixed by the magnetic symmetry. The couplings inside the hexamers are only partly fixed by symmetry. The couplings between different copper spin pairs formed by Cu1, Cu2, and Cu3 positions are not fixed by symmetry and should be found from the fits to the experimental data. The coupling inside each Cu pair is FM in the *ac* plane and AFM along the *b* axis because the spins in the pair are related by primed 2-fold axis $2'_y$. One can go down to lower symmetry by mixing the irreps mGM2− and mGM2+, resulting in the subgroup C2'. In this group the intrahexamer coupling remains the same, but the second hexamer becomes independent, doubling the number of free parameters to 18. If one adds additionally irrep mGM1+, then the symmetry relations between all 24 atoms in both hexamers disappear in the MSG P1.

The basis transformation to the P2_1/c.1'_C[C2/c] 14.84 (mY2−) MSG structure is the identity matrix with the origin shift (1/4, 1/4, 0). Similarly to the C2'/c MSG, the hexamers are completely related by symmetry. Technically, by symmetry operators, the pairs in the hexamers are constructed differently. The inversion −1 relates the spins on different hexamers as before, but the twofold screw axis 2_1 now relates the spins in the different hexamers as well. The second spin in each pair is generated by the time-odd centering translation 1'_C operator.

Although the accepted standard symbol and settings of the MSG is UNI, which combines a modified BNS symbol with essential information from the Opechowski-Guccione (OG) symbol [16,23], we like to give also the description of this MSG in the OG setting, which is, in our view, more physically relevant here. In this setting there is no origin shift from the parent group and the MSG OG symbol reads C_P2'/c. So the Cu spins in the Cu pairs generated by noncentered operators have exactly the same configuration as for C2'/c, but the pairs related by C-centering are time-reversal odd due to OG propagation vector $\boldsymbol{k} = [0, 1, 0]$. Finally the only difference of the magnetic structures in OG settings is that the hexamers related by the centering translations (1/2, 1/2, 0)+ are coupled AFM in the sample with A = Na, but not FM as in the samples with A_2 = K$_2$ and NaK (Fig. 7).

Interestingly, there is another different magnetic structure in the same MSG (No. 14.84) but generated by the parity even irrep mY2+. This structure is derived from the parent gray space group by different basis transformation and in spite of the same symmetry elements the magnetic structure is different. This emphasizes the importance of specifying the new atomic positions in the MSG if the basis transformation is not given.

B. Magnetic structure determination

As a first step, using the FULLPROF program, we have performed a simulated annealing (SA) search [15,24] of the full diffraction profile for the models described in the previous sections. A SA search starts from random values of the free parameters and we have repeated the search more than

TABLE II. The magnetic model parameters for $A_2Cu_3O(SO_4)_3$ (A_2 = K$_2$, NaK, Na$_2$) refined from the diffraction data shown in Figs. 8–10. The numeration of the atoms is as indicated in Table I. Here M is the size of the magnetic moment, ϕ and θ are spherical angles with c and b axes, respectively, m_x, m_y, and m_z are respective magnetic moment projections in the MSGs C2'/c for A_2 = K$_2$, NaK and P2_1/c.1'_C[C2/c] (UNI) for A = Na. The error bars are given only for the refined parameters. The reliability factors [15] R_p, R_{wp}, R_{exp}, χ^2 are shown as the bottom line for each type of fit. Three models are presented: (A) the most general fit (see text for details); (B) the Cu1 and Cu2 moment sizes and spherical angle are constrained to be the same; (C) all moments are constrained to be parallel in the hexamers. The magnetic crystallographic information (mcif) files for LSQ fits (model A) can be found in the Supplemental Material [20].

	K			NaK			Na		
	M (μ_B)	ϕ	θ	M (μ_B)	ϕ	θ	M (μ_B)	ϕ	θ
	m_x	m_y	m_z	m_x	m_y	m_z	m_x	m_y	m_z
Le Bail model-free fit									
$R_p, R_{wp}, R_{exp}, \chi^2$	6.15, 5.88, 4.65, 1.60			6.06, 6.91, 7.03, 0.966			6.00, 6.29, 5.32, 1.40		
Simulated annealing (SA)									
Cu1	0.577	339.496	106.484	0.618	321.624	89.727	0.762	198.214	108.667
	−0.207	−0.164	0.446	−0.420	0.003	0.314	−0.243	−0.244	−0.776
Cu2	0.459	339.118	104.214	0.618	343.403	118.547	0.512	180.205	125.251
	−0.169	−0.113	0.356	−0.170	−0.295	0.451	−0.002	−0.295	−0.418
Cu3	0.433	161.513	92.706	0.571	185.893	89.278	0.472	236.501	94.796
	0.146	−0.020	−0.359	−0.064	0.007	−0.594	−0.423	−0.040	−0.417
$R_p, R_{wp}, R_{exp}, \chi^2$	6.45, 6.04, 4.65, 1.69			6.57, 7.61, 7.03, 1.17			6.51, 6.70, 5.32, 1.59		
Model A. Least square fit (LSQ)									
Cu1	0.593(28)	349(10)	112.0(5.6)	0.617(53)	325.6(9.9)	93.1(6.0)	0.731(42)	198.5(5.6)	105.6(7.7)
	−0.1(1)	−0.222(59)	0.503(60)	−0.4(1)	−0.034(66)	0.4(1)	−0.241(75)	−0.2(1)	−0.757(43)
Cu2	0.434(40)	345(13)	98.0(7.4)	0.581(83)	350.2(9.3)	119.4(6.2)	0.493(53)	183.9(8.8)	121.4(9.4)
	−0.1(1)	−0.060(56)	0.374(53)	−0.095(89)	−0.285(73)	0.460(88)	−0.031(68)	−0.256(90)	−0.431(32)
Cu3	0.442(21)	180	90	0.532(51)	188(11)	87(26)	0.480(18)	240.3(5.6)	90
	0	0	−0.442(21)	−0.1(1)	0.0(2)	−0.561(70)	−0.449(35)	0	−0.405(29)
$R_p, R_{wp}, R_{exp}, \chi^2$	6.47, 5.96, 4.55, 1.71			6.64, 7.40, 6.84, 1.17			6.57, 6.61, 5.19, 1.62		
Model B. Least square fit (LSQ) Cu1 and Cu2 are constrained									
Cu1	0.527(15)	339.0(3.5)	105.8(1.2)	0.574(25)	339.7(7.8)	104.8(3.0)	0.586(20)	184.4(3.9)	115.6(3.0)
	−0.194(31)	−0.143(11)	0.406(25)	−0.210(77)	−0.146(32)	0.435(63)	−0.043(39)	−0.253(34)	−0.543(20)
Cu2	0.527(15)	339.0(3.5)	105.8(1.2)	0.574(25)	339.7(7.8)	104.8(3.0)	0.586(20)	184.4(3.9)	115.6(3.0)
	−0.194(31)	−0.143(11)	0.406(25)	−0.210(77)	−0.146(32)	0.435(63)	−0.043(39)	−0.253(34)	−0.543(20)
Cu3	0.422(31)	160.2(7.3)	96(32)	0.526(53)	192(11)	97(53)	0.486(25)	230.6(5.8)	94(24)
	0.152(52)	−0.0(2)	−0.342(44)	−0.1(1)	−0.1(5)	−0.559(72)	−0.404(41)	−0.0(2)	−0.458(26)
$R_p, R_{wp}, R_{exp}, \chi^2$	6.76, 7.49, 6.90, 1.18			6.76, 7.49, 6.90, 1.18			6.84, 6.85, 5.22, 1.72		
Model C. Least square fit (LSQ) Cu1 and Cu2 and Cu3 are constrained to be (anti)parallel									
Cu1	0.469(10)	320.2(3.4)	90	0.595(17)	327.3(5.1)	90	0.524(14)	158.7(4.1)	90
	−0.320(22)	0	0.249(28)	−0.351(45)	0	0.358(54)	0.205(38)	0	−0.411(30)
Cu2	0.469(10)	320.2(3.4)	90	0.595(17)	327.3(5.1)	90	0.524(14)	158.7(4.1)	90
	−0.320(22)	0	0.249(28)	−0.351(45)	0	0.358(54)	0.205(38)	0	−0.411(30)
Cu3	−0.477(11)	320.2(3.4)	90	−0.395(29)	327.3(5.1)	90	0.469(20)	158.7(4.1)	90
	0.325(26)	0	−0.253(26)	0.233(45)	0	−0.238(26)	0.184(33)	0	−0.368(31)
$R_p, R_{wp}, R_{exp}, \chi^2$	7.56, 7.24, 4.60, 2.48			7.40, 8.35, 6.96, 1.44			7.12, 7.57, 5.26, 2.07		

several hundred times. The search was performed for all three samples. The results of the SA search are listed in Table II and the illustrations of the magnetic structures corresponding to the SA part in the table are shown in Fig. 7. Note that the parameters found in the SA search do not have error bars.

Based on the values from the SA search, we have performed standard Rielveld least square (LSQ) refinement. Figures 8–10 show the LSQ fits of the difference diffraction patterns. Although the magnetic structures that we have found are similar for the samples with A_2 = K$_2$ and NaK, the

diffraction patterns have different distribution of the intensities over the Bragg peaks. For instance, the first Bragg peak (001) at $2\theta \simeq 20$ degrees has different relative intensity in comparison with the main group of peaks in the middle of the pattern around $2\theta \simeq 70$ degrees. The sample with A = Na has a completely different diffraction pattern; e.g., the first peak has zero intensity.

For all samples we present three types fits in Table II: (A) the most general fit, all parameters are independent; (B) the Cu1 and Cu2 moment sizes and spherical angles are
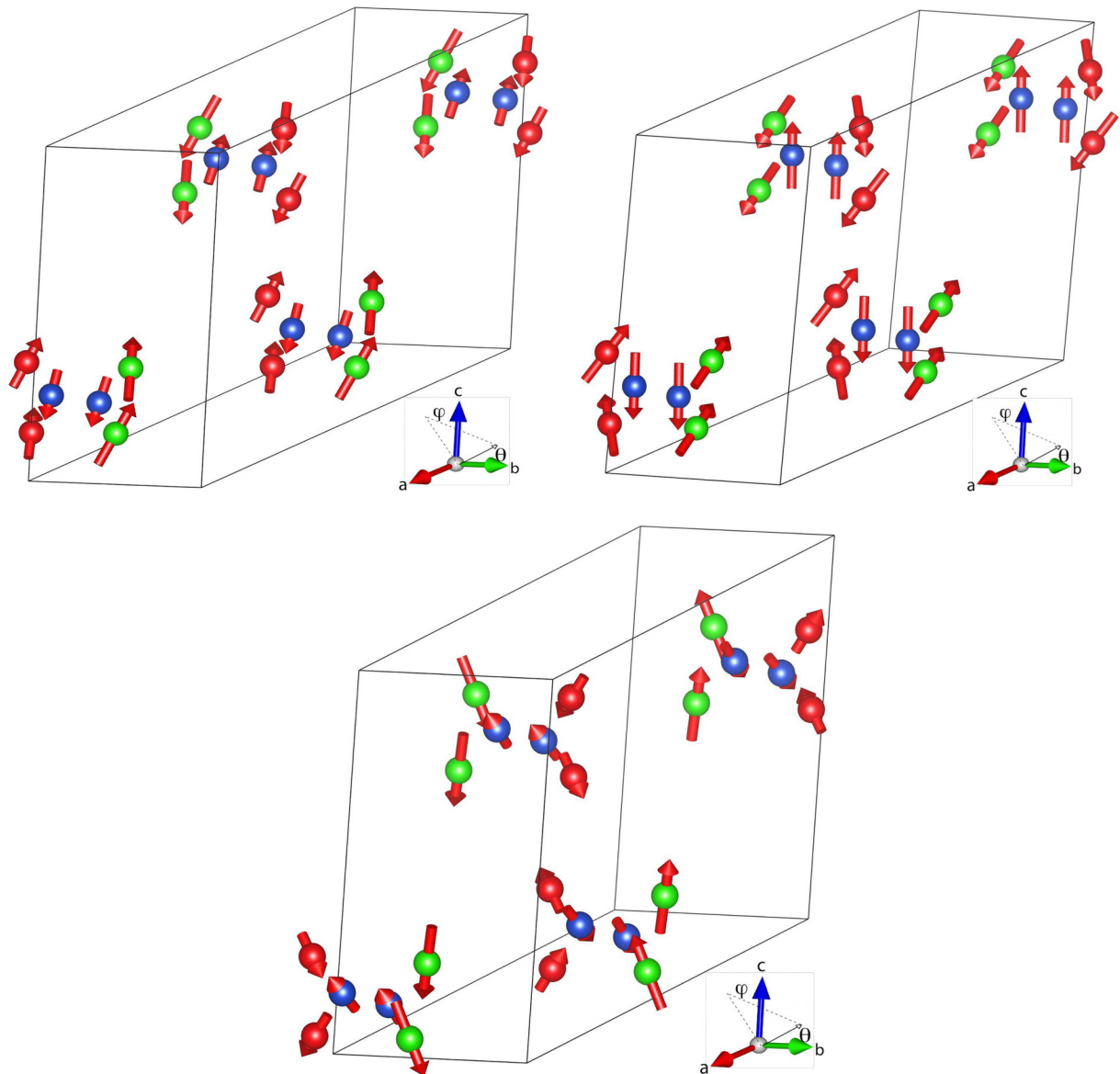
FIG. 7. The magnetic structures formed by the hexamers in MSGs (top) C2'/c and (bottom) P2_1/c.1'_C[C2/c] (UNI symbol [23]) or C_P2'/c (OG symbol). The number of atoms is 24 in one unit cell, but some atoms are shown outside the unit cell to better represent the four hexamers. The hexamers related by inversion in C2'/c settings along *bc* diagonal (those that are closest and that are arranged approximately in vertical direction in the figure) are coupled AFM. Two other hexamers related by C-centering translation (1/2, 1/2, 0) are coupled FM for the samples with $A_2 = K_2$ and NaK (left and right top structures), but AFM coupled for the sample with $A = $ Na (bottom). The side spin pairs Cu1 and Cu2 are in green and red; the central Cu3 pair is in blue.

constrained to be the same; (C) all moments are constrained to be aligned (anti)parallel in the hexamers, like in the theoretical model of isolated trimer considered in Sec. IV. For the sample with $A = $ K, the fit A had to be constrained to get a convergent result: the middle spin Cu3 angles are fixed to $\theta = 90$ degrees and $\phi = 90$ degrees, leaving only the z component of the Cu3 spin to be nonzero.

VI. DISCUSSION

We have synthesized and studied the crystal and magnetic structures of the compounds $A_2Cu_3O(SO_4)_3$ ($A_2 = $ Na$_2$, NaK, K$_2$). Crystallographically, the $S = 1$ copper hexamers form a two-dimensional network in the *bc* plane, but

three-dimensional long-range magnetic order is observed below T_N. Surprisingly, there are differences in the long-range magnetic order: the compounds with $A_2 = $ NaK and $A = $ K are ordered in the Shubnikov magnetic space group (MSG) C2'/c, whereas in the compound with $A = $ Na the MSG is P2_1/c.1'_C[C2/c] in standard UNI notation, as explained in Sec. V A. Here for the comparison of the two structures we prefer to use Opechowski-Guccione (OG) notation [11]. In this notation, both groups C2'/c and C_P2'/c keep the parent space group metrics and have the same set of symmetry operators for noncentered atoms, but the atoms related by centering translations (1/2, 1/2, 0)+ are FM coupled in C2'/c and AFM in C_P2'/c. In both groups, the copper spins in Cu pairs are related by symmetry and coupled FM for
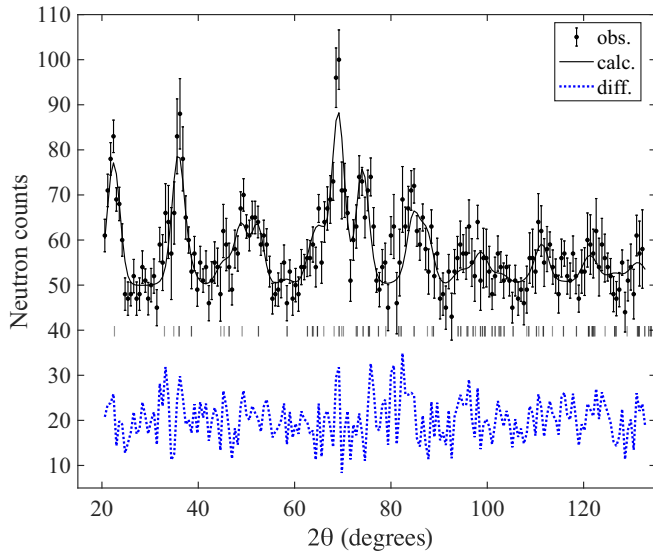
FIG. 8. The fit to C2'/c model of the difference pattern for the sample $A_2Cu_3O(SO_4)_3$ (A_2 = NaK) containing purely magnetic contribution, measured at CNCS/SNS with the wavelength $\lambda = 4.96$ Å. The row of tick marks shows the Bragg peak positions. The difference between the observed and calculated intensities is shown by the dotted blue line.

FIG. 9. The fit to C2'/c model of the difference pattern for the sample $A_2Cu_3O(SO_4)_3$ (A = K) containing purely magnetic contribution, measured at CNCS/SNS with the wavelength $\lambda = 4.96$ Å. The row of tick marks shows the Bragg peak positions. The difference between the observed and calculated intensities is shown by the dotted blue line. The reliability factors [15] R_p, R_{wp}, R_{exp}, χ^2 are 6.45, 6.04, 4.65, 1.69.

FIG. 10. The fit to the model P2_1/c.1'_C[C2/c] [basis transformation from parent (1,0,0), (0,1,0), (0,0,1); 1/4, 1/4, 0] of the difference pattern for the sample $A_2Cu_3O(SO_4)_3$ (A = Na) containing purely magnetic contribution, measured at CNCS/SNS with the wavelength $\lambda = 4.96$ Å. The row of tick marks shows the Bragg peak positions. The difference between the observed and calculated intensities is shown by the dotted blue line.

spin components in the *ac* plane and AFM along the *b* axis. Figure 7 shows the magnetic structures for all three compounds with the simulated annealing values from Table II. As one can see from Table II and Fig. 7, the largest spin component is along the *z* axis that makes the Cu pairs approximately FM aligned. The n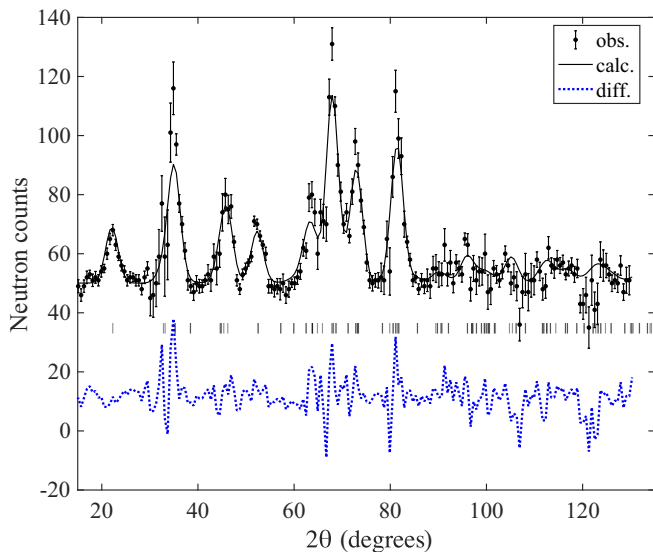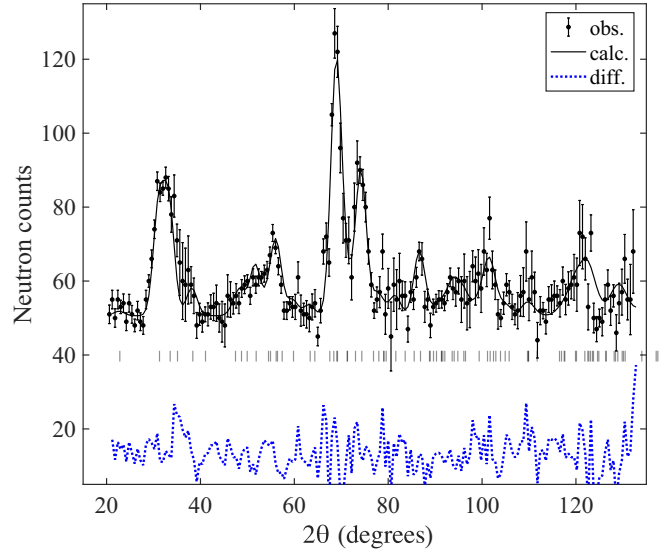eighboring pairs in the hexamers are approximately AFM coupled, and this coupling is not dictated by symmetry, but is a result of the fits of the experimental data. In addition to the general fit A, there are two types of the constrained fits presented in Table II. The fit B constraining the side spins Cu1 and Cu2 does not make the spins strictly parallel, due to the symmetry element 2_y' in the C2'/c MSG. Namely, the nonzero *y* components make the pairs of Cu-Cu in the hexamer related by the 2_y' nonparallel. However, one can see from the fit B that the *y* components of all three atoms are the smallest ones, so we have attempted to use yet more restricted model C with the zeroed *y* components of all magnetic moments forcing collinear alignments of all spins in the hexamer. This type of fit yields a noticeable degradation of the fit, e.g., χ^2 becomes twice as large for the sample with A = K, so we can conclude that noncollinearity and frustration can be inferred from the diffraction data. Figure 11 further illustrates the spin directions in two projections for the sample with A = K. The *ac* and *bc* projections nicely demonstrate the couplings and magnetic moment directions. One can also see that the centered hexamers are FM coupled in the *ab* projection.

The ground state is expected to be the triplet with FM coupling in the Cu pairs and AFM between neighboring Cu pairs as was shown in Sec. IV. As discussed above, the main spin components are in accordance with this type of coupling. However the presence of the noncollinear components of the magnetic moments within the Cu hexamers gives evidence for spin frustration. We think that the origin of the noncollinear spin arrangement results from a compromise to handle possible spin frustrations within the weak interhexamer interactions. From the isolated hexamer calculations, we have the magnetic moments 0.79, 0.70, and 0.49 μ_B (using g
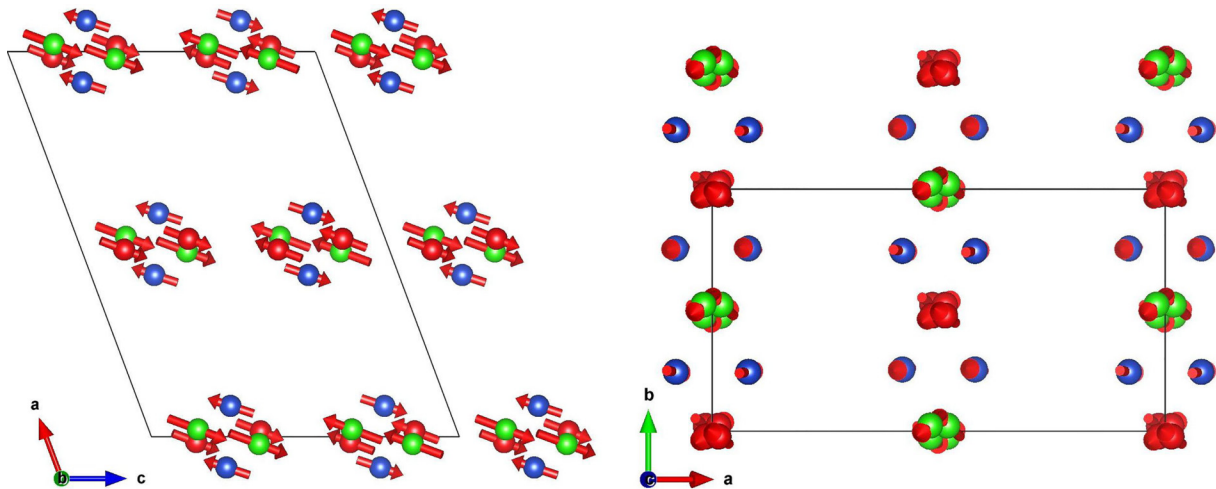
FIG. 11. The magnetic structure in the sample with $A = $ K (C2'/c) in two projections. The ac and bc layers are FM stacked along the b- and a-axis directions, respectively. The side spin pairs Cu1 and Cu2 are in green and red; the central Cu3 pair is in blue.

factor 2) for the end positions Cu1, Cu2 and the middle Cu3. The sizes of the magnetic moments are expectedly smaller than the Cu^{2+} ion value of 1 μ_B due to quantum entanglement in the wave function in hexamer. Experimentally we have the following values of the Cu1, Cu3, and Cu2 magnetic moment sizes for $A = $ K: 0.59(3), 0.44(2), 0.43(4), $A_2 = $ NaK: 0.62(5), 0.53(5), 0.58(8), $A = $ Na: 0.73(4), 0.48(2), 0.49(5) in μ_B. We find that this is a fairly good correspondence between the experiment and the calculations in the simple model disregarding the interhexamer interaction. In particular, for the middle pair Cu3 the calculated moment 0.49 μ_B is practically within the experimental error bars. The side Cu1 and Cu2 pairs have experimentally smaller values (by maximum 26% and 39% smaller in the sample with $A = $ K) than expected from the isolated hexamer. This is not surprising because the strongest interhexamer interactions that can modify the spin expectation values are between the end-standing Cu spins as discussed below.

Nekrasova *et al.* performed *ab initio* calculations to estimate the intrahexamer and interhexamer superexchange interactions and the anisotropy for the hexamer molecule [9]. The strongest calculated intrahexamer interactions of type Cu-O-Cu are in amazingly good agreement with the results derived directly from neutron spectroscopy INS experiments [6,8,10]. The two smallest interactions in the end-standing Cu1-Cu1 and Cu2-Cu2 pairs are calculated to be antiferromagnetic in contradiction with the INS experiments, where these two couplings were found to be ferromagnetic [25]. In principle, the FM sign of the intrahexamer interactions of type Cu-O-Cu in Cu pairs is consistent with the Goodenough-Kanamori-Anderson rules. Unfortunately the above *ab initio* calculations did not show the spin expectation values, which could then be compared with the experimental values from the present diffraction data and with our calculations for the isolated hexamers in the mean field.

Figure 12 shows five hexamers in the magnetic structure in the K sample with several bonds between Cu atoms indicated by black arrows. The blue dashed arrows show the symmetry relations between the hexamers. One hexamer from the neighboring cell shifted by (0,1,0) is shown to better visualize

the bonding. The hexamers along the a, b, and c directions are always FM-arranged because they are separated by integer lattice translations and the k vector is zero or one. These distances between the Cu spins are very large, about 19 and 14 Å for the a and b directions. However, since the hexamer is elongated mainly along the b direction the interdistances between
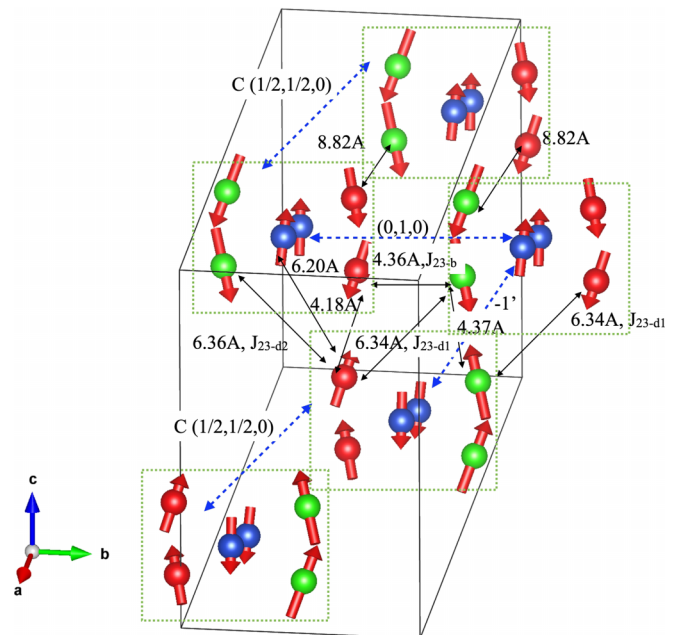

FIG. 12. The magnetic structure in the sample with $A = $ K (C2'/c) showing the connectivity between hexamers. Each hexamer unit is outlined by dashed green box. The side spin pairs Cu1 and Cu2 are in green and red; the central Cu3 pair is in blue. The black arrows indicate the bonds between side hexamer spins Cu1 and Cu2 of different hexamers. Three bonds are labeled in the notation from Ref. [9]. Five hexamers are shown with the transforming symmetry operations indicated by the blue dashed lines. The hexamers that are AFM coupled are related by inversion $-1'$. The ones that are FM coupled are related by C-centering (1/2, 1/2, 0) or just translation (0,1,0).

Cu1 and Cu2 from neighboring hexamers along the *b* axis are small, about 4.36 Å, as shown in Fig. 12 and labeled as J_{23-b} following the notation [9]. The hexamers along the *ab*, *bc*, and *ac* diagonals belong to the same unit cell and their coupling depends on the specific magnetic symmetry. The *ab initio* calculations give zero coupling along the *b* axis [9], which contradicts the ferromagnetic couplings obtained from the analysis of the magnetic excitation spectra [10]. Experimentally, we have FM arrangement in this direction, as explained above. The *ab initio* calculations predict the strongest AFM couplings along the diagonals in the *bc* plane as indicated in Fig. 12 by the J_{23-d1} and J_{23-d2} bonds. This diagonal *bc* coupling is indeed AFM as observed experimentally for all three compounds, and these are the bonds between Cu1 and Cu2 atoms in the hexamers belonging to the same unit cell and related by inversion. The AFM coupling along the *bc* diagonal is also well seen in Fig. 11. The hexamer spin arrangement along the *ab* diagonal is given by C-centering translation, and it is FM for $A_2 = K_2$, NaK as one can see in Fig. 11 and AFM for $A = $ Na. As a consequence the arrangement along the *ac* diagonal is AFM in the samples with $A_2 = K_2$ and NaK and FM in the sample with $A = $ Na. In general, all interhexamer coupling in all three samples is protected by magnetic symmetry. The difference in the magnetic ordering in the sample with $A = $ Na is apparently due to different coupling along *ab* and *ac* diagonals. These couplings are independent from the coupling along the *bc* diagonal. It would be interesting to compare them with the *ab initio* theoretical calculations to see the reason for the different coupling sign. The fact that the lattice parameter ratios a/b and a/c for $A = $ Na differ by almost 10% from those for $A = $ K and $A_2 = $ NaK may be indicative of the interhexamer couplings in $A = $ Na being different from those in $A = $ K and NaK.

The very new point of our study is the experimental determination of the magnetic structures in Cu-hexamer cluster systems, which so far were unknown. It would be interesting to compare with literature results for other magnetic systems containing Cu clusters. There are many inorganic materials in which coupled Cu-spin dimers can be found, such as $KCuCl_3$ and $TlCuCl_3$, malachite $Cu_2CO_3(OH)_2$, callaghanite $Cu_2Mg_2(CO_3)(OH)_6 \cdot 2H_2O$, and urusovite $CuAl(AsO_4)O$, discussed in a review [2]. None of them has 3D magnetic ordering in zero magnetic field. Copper-based molecular magnets such as coordination polymers and metal-organic frameworks often contain Cu spin clusters in their structures, for instance spin dimers in three complexes $Cu_2(oxen)(PYNN)_2(ClO_4)_2$ (PYNN = o-, m-, and p-pyridyl nitronyl nitroxide) [26]. Similarly to inorganic Cu-dimer systems, none of them shows long-range magnetic order according to magnetic susceptibility data. On the other hand, spin-trimer clusters such as $A_3Cu_3(PO_4)_4$ ($A = $ Ca, Sr, Pb) [27,28] and $Ca_3Cu_{3-x}Ni_x(PO_4)_4$ [29] are in the nonsinglet state and exhibit long-range magnetic ordering at low temperatures. An interesting arrangement of Cu tetramers in molecular cubes of Cu_4O_4 or Ni_4O_4 can be constructed by condensation reactions of aldehyde and aminoalkyl alcohol with Schiff base ligands resulting in organic compounds $[Cu_4(Hhsae)_4] \cdot 2H_2O \cdot 4CH_3CN$ and $[Ni_4(sae)_4(MeOH)_4]$ [30]. Both tetramer systems have high-spin ground states and are ordered magnetically according to magnetic susceptibility data. The Cu-tetramer units in inorganic olivenite $Cu_2(AsO_4)(OH)$ and libethenite $Cu_2(PO_4)(OH)$, also considered in the above mentioned review [2], do not show any long-range magnetic order down to 1.8 K being in a spin-singlet ground state. A peculiar crystal of the heterometal Cu_6Fe wheel molecules in organic compound $[(Cu_6^{II}Fe^{III})(HL)_6-(OH)_2(OCH_3)_4](NO_3)_3 \cdot 6H_2O$ was reported in [31]. The heptanuclear wheel cluster consists of a central Fe ion surrounded by six Cu ions, linked through methoxo- and hydroxo-bridges. Six magnetically isolated Cu(II) ions ($S = 1/2$) and one high-spin Fe(III) ion ($S = 5/2$) are AFM coupled. Larger magnetic clusters that consist of more than six spins can also be found [2]. Unlike the smaller Cu-cluster systems, the large magnetic clusters usually do not develop a long-range magnetic order. Instead, the ground state is protected by an energy barrier for spin reversal [2]. For example the Cu_{24} clusters in the boleite with the formula $KPb_{26}Ag_9Cu_{24}(OH)_{48}Cl_{62}$ or cuboctahedral Cu_{12} clusters in the tschörtnerite $Ca_4(K,Ca,Sr,Ba)_3Cu_3Al_{12}Si_{12}O_{48}(OH)_8 \cdot 20H_2O$ both result in a singlet ground state of the whole cluster.

VII. CONCLUSIONS

The crystal and magnetic structures of the spin $S = 1$ hexamer cluster $A_2Cu_3O(SO_4)_3$ (fedotovite $A_2 = K_2$, euchlorine NaK, puninite Na_2) were studied by neutron powder diffraction at temperatures 1.6–290 K. The crystal structures in all compounds are well refined in the monoclinic space group C2/c (No. 15), whereas the magnetic structures are different with the magnetic space groups (MSGs) 15.87 C2'/c for $A_2 = K_2$, NaK and 14.84 P2_1/c.1'_C[C2/c] for $A = $ Na. The basic magnetic units of the compounds are strongly coupled pairs of Cu in quasi-isolated copper hexamers, which are coupled to each other by weak superexchange interactions. The interhexamer interactions are completely fixed by MSGs. The coupling of the Cu spins in pairs is fixed by MSG symmetry, whereas the interpair coupling is not symmetry related. Experimentally we found that the pairs are approximately ferromagnetically FM coupled in pairs and antiferromagnetically AFM between neighboring pairs. The magnetic moment sizes of the side pairs Cu1, Cu2 and the middle Cu3 spins amounted to 0.59(3), 0.43(4), 0.44(2) for $A = $ K, 0.62(5), 0.58(8), 0.53(5) for $A_2 = $ NaK, and 0.73(4), 0.49(5), 0.48(2) for $A = $ Na in μ_B. The coupling and the moment sizes are in good agreement with the model calculations for the isolated hexamers in the mean field with Hamiltonian parameters from inelastic neutron scattering (INS) studies [6,8,10]. The ground state is a triplet for the Hamiltonian with FM in pairs and AFM interpair coupling, with the spin expectation values $\langle s \rangle$ independent of the exchange constants being $2\langle s \rangle = 3/4 \ \mu_B$ for the end pairs and $1/2 \ \mu_B$ for the middle pair. For more refined exchange parameters, the $2\langle s \rangle$ values are the same within the accuracy 0.005 μ_B for all three samples, being 0.79, 0.70, 0.49 μ_B for the side pairs Cu1, Cu2 and the middle pair Cu3 magnetic moments.

ACKNOWLEDGMENTS

[1] S. Sachdev, Nat. Phys. **4**, 173 (2008).

[2] D. S. Inosov, Adv. Phys. **67**, 149 (2018).

[3] M. R. Norman, Rev. Mod. Phys. **88**, 041002 (2016).

[4] M. Fujihala, T. Sugimoto, T. Tohyama, S. Mitsuda, R. A. Mole, D. H. Yu, S. Yano, Y. Inagaki, H. Morodomi, T. Kawae, H. Sagayama, R. Kumai, Y. Murakami, K. Tomiyasu, A. Matsuo, and K. Kindo, Phys. Rev. Lett. **120**, 077201 (2018).

[5] J. Strecka and K. Karlova, AIP Adv. **8**, 101403 (2018).

[6] A. Furrer, A. Podlesnyak, E. Pomjakushina, and V. Pomjakushin, Phys. Rev. B **98**, 180410(R) (2018).

[7] M. Hase, K. C. Rule, J. R. Hester, J. A. Fernandez-Baca, T. Masuda, and Y. Matsuo, J. Phys. Soc. Jpn. **88**, 094708 (2019).

[8] A. Furrer, A. Podlesnyak, J. M. Clemente-Juan, E. Pomjakushina, and H. U. Güdel, Phys. Rev. B **101**, 224417 (2020).

[9] D. O. Nekrasova, A. A. Tsirlin, M. Colmont, O. Siidra, H. Vezin, and O. Mentré, Phys. Rev. B **102**, 184405 (2020).

[10] A. Furrer, A. Podlesnyak, E. Pomjakushina, and V. Pomjakushin, Phys. Rev. B **104**, L220401 (2021).

[11] D. B. Litvin, 1-, 2- and 3-dimensional magnetic subperiodic groups and magnetic space groups, *Magnetic Group Tables* (International Union of Crystallography, Chester, 2013), https://www.iucr.org/publ/978-0-9553602-2-0.

[12] A. P. Ramirez, Annu. Rev. Mater. Sci. **24**, 453 (1994).

[13] G. Ehlers, A. A. Podlesnyak, J. L. Niedziela, E. B. Iverson, and P. E. Sokol, Rev. Sci. Instrum. **82**, 085108 (2011).

[14] P. Fischer, G. Frey, M. Koch, M. Koennecke, V. Pomjakushin, J. Schefer, R. Thut, N. Schlumpf, R. Buerge, U. Greuter, S. Bondt, and E. Berruyer, Physica B: Condens. Matter **276-278**, 146 (2000).

[15] J. Rodriguez-Carvajal, Physica B: Condens. Matter **192**, 55 (1993).

[16] B. J. Campbell, H. T. Stokes, D. E. Tanner, and D. M. Hatch, J. Appl. Cryst. **39**, 607 (2006).

[17] H. T. Stokes, D. M. Hatch, and B. J. Campbell, ISOTROPY Software Suite, https://iso.byu.edu.

[18] M. Aroyo, J. Perez-Mato, D. Orobengoa, E. Tasci, G. de la Flor, and A. Kirov, Bulg. Chem. Commun. **43**, 183 (2011).

[19] J. M. Perez-Mato, S. V. Gallego, E. S. Tasci, L. Elcoro, G. de la Flor, and M. I. Aroyo, Annu. Rev. Mater. Res. **45**, 217 (2015).

[20] See Supplemental Material at http://link.aps.org/supplemental/10.1103/PhysRevB.109.144409 for three mcif files with crystallographic information about crystal and magnetic structures.

[21] G. L. Starova, S. K. Filatov, V. S. Fundamensky, and L. P. Vergasova, Mineral. Mag. **55**, 613 (1991).

[22] F. Scordari and F. Stasi, Neues Jahrbuch für Mineralogie-Abhandlungen **161**, 241 (1990).

[23] B. J. Campbell, H. T. Stokes, J. M. Perez-Mato, and J. Rodríguez-Carvajal, Acta Crystallogr., Sect. A **78**, 99 (2022).

[24] S. Kirkpatrick, C. D. Gelatt, and M. P. Vecchi, Science **220**, 671 (1983).

[25] The signs of $J_{neutron}$ in Ref. [9] (Table II) for the end pairs for $A = K$ are reversed in comparison with the original paper [8]. The sizes of $J_{neutron}$ are correct. The numeration of Cu in the hexamer is different from the one in present paper.

[26] Z. Liu, Z. Lu, D. Zhang, Z. Jiang, L. Li, C. Liu, and D. Zhu, Inorg. Chem. **43**, 6620 (2004).

[27] A. A. Belik, A. Matsuo, M. Azuma, K. Kindo, and M. Takano, J. Solid State Chem. **178**, 709 (2005).

[28] M. Drillon, M. Belaiche, P. Legoll, J. Aride, A. Boukhari, and A. Moqine, J. Magn. Magn. Mater. **128**, 83 (1993).

[29] V. Y. Pomjakushin, A. Furrer, D. V. Sheptyakov, E. V. Pomjakushina, and K. Conder, Phys. Rev. B **76**, 174433 (2007).

[30] T. Shiga and H. Oshio, Sci. Technol. Adv. Mater. **6**, 565 (2005).

[31] R. Saiki, N. Yoshida, N. Hoshino, G. N. Newton, T. Shiga, and H. Oshio, Chem. Lett. **46**, 1197 (2017).